2018

Change in Working Length at Different Stages of Instrumentation as a Function of Canal Curvature

Mei Tang

Virginia Commonwealth University

Change in Working Length at Different Stages of Instrumentation as a Function of Canal Curvature

A thesis submitted in partial fulfillment of the requirements for the degree of Master of Science in Dentistry at Virginia Commonwealth University

by

Mei I Tang
DMD, University of Pittsburgh School of Dental Medicine, 2014
BS, University of California at Davis, 2008

Director: Dr. Garry L. Myers, DDS
Program Director, Advanced Education Program in Endodontics

Virginia Commonwealth University
Richmond, Virginia
May 2018

Table of Contents

List of Tables

List of Figures

Abstract

Change in Working Length at Different Stages of Instrumentation
as a Function of Canal Curvature

By Mei I Tang, DMD

A thesis submitted in partial fulfillment of the requirements for the degree of Master of Science in Dentistry at Virginia Commonwealth University.

Virginia Commonwealth University, 2018

Director: Dr. Garry Myers, DDS
Program Director, Advanced Education Program in Endodontics

The aim of this study was to determine the change in working length (ΔWL) before and after coronal flaring and after complete rotary instrumentation as a function of canal curvature. One mesiobuccal or mesiolingual canal from each of 43 extracted molars had coronal standardization and access performed. Once the access was completed, canal preparation was accomplished using Gates Glidden drills for coronal flaring and EndoSequence files for rotary instrumentation. WLs were obtained at 3 time points: pre-instrumentation (unflared), mid-instrumentation (flared) and post-instrumentation (concluded). Measurements were made via direct visualization (DV) and the CanalPro apex locator (EM) in triplicate by a single operator with blinding across the time points. Root curvature was measured using Schneider's technique. The change in working length was assessed using repeated-measures ANCOVA. The direct visualization measurements were statistically larger than the electronic measurements (paired t-test difference = 0.20 mm, SE = 0.037, $P < .0001$), although a difference this large may not be clinically important. Overall, a greater change in working length was observed in straight canals than in curved canals. This unexpected finding was attributed to the limitations of the study,

specifically the confounding factor of root length. This trend was more pronounced when measured electronically than via direct visualization, especially after complete instrumentation than after coronal flaring. The overall change in working length after complete instrumentation was found to be clinically insignificant in this study. A limited amount of change in working length may be expected prior to obturation.

Introduction

Working length determination is a fundamental step in the biomechanical preparation of the root canal system which directly impacts treatment outcome. Many studies have shown that the prognosis of periapical healing is associated with the length of obturation. Davis et al, in a histological study using a dog model, demonstrated that underfilled canals could have successful re-establishment of healthy periodontal tissue if the canal was prepared to the apex, while overfilling caused advanced destruction and liquefaction necrosis of the periodontal tissue.(1) In a twenty-year retrospective chart review, Swartz et al found that overfilled cases had a failure rate that was four times higher than underfilled cases.(2) Ricucci's literature review on length of fill found greatest success at 90% to 94% in cases with short fills.(3) In a systematic review of outcome studies, Ng et al identified length of obturation within 2 mm from working length as one of the four important factors for endodontic success.(4, 5) Sjogren et al evaluated endodontic outcomes at 8 to 10 years and found a success rate of 94% for obturation length within 2 mm short of apex, 76% for overfill and 68% for underfill greater than 2 mm.(5)

The subject of length of obturation in relation to apical anatomy has been greatly studied. Two important landmarks in the anatomy of the root apex are the major apical foramen and the minor apical foramen; the latter is also known as the apical constriction. It has been demonstrated that the anatomic apex and the major foramen do not always coincide. Classic studies by Kuttler and Green demonstrated that the apical foramen is located 1-2 mm from the root apex in over 50% of teeth.(6, 7) Burch and Hulen found the frequency of deviation of the major foramen from the anatomic apex to be as high as 98.9%, with an average deviation of 0.59 mm.(8) In a micro-CT study by ElAyouti et al, the average distance between the apex and the apical foramen was found to be 0.9 mm.(9) The apical constriction has traditionally been

advocated to be the termination point of endodontic therapy. It has been described as a natural narrowing of the root canal space usually in close proximity to the cementodentinal junction (CDJ), a histological location beyond which tissue is periodontal.(10, 11) In a study by Kuttler, the location of the apical constriction was found to vary with age as a result of cementum deposition; the constriction was located at a distance of 0.524 mm from the apical foramen in those aged 18 to 25 years, and 0.659 mm in those aged 55 years and above.(6) The existence of the apical constriction has been discussed in the literature. Meder-Cowherd et al has shown in a micro-CT study of palatal roots of maxillary molars that the traditional infundibular shape of the apical constriction was absent in 65% of cases, contending that the apical constriction could not be tactilely determined.(12) On the other hand, a CBCT study by ElAyouti et al found the apical constriction to be present 100% of the time, with 76% of the apical constriction being parallel and only 10% having the traditional infundibular shape.(9) Regardless of the controversy, most endodontists limit the extent of obturation to the region of the apical constriction at 0.5 to 1 mm from the apical foramen, based on the findings of the aforementioned classic studies.

Historically, working length determination was achieved by radiographs alone. However, there are several limitations to this modality. Firstly, radiographic images are prone to distortion due to angulation of film placement.(13) Secondly, it is often difficult to determine the exact position of the apical foramen radiographically. Root curvature in a buccolingual direction may not allow accurate interpretation of the anatomic apex.(14) Superimposition with natural anatomic structures increases difficulty of image interpretation.(15) As previously mentioned, the apical foramen also frequently deviates from the anatomic apex.(7, 16) Williams et al found a significant difference in working length measurements obtained by periapical radiographs clinically and microscopic measurement after extraction of the same tooth. He found that the

length of the file was always longer than what appeared radiographically.(17) Stein and Corcoran reported the radiographic position of the file to be 0.7 mm shorter than its actual position.(18) ElAyouti et al found that radiographic working length that was 0 to 2 mm short of the apex caused unintentional over-instrumentation in 51% of premolars and 22% of molars.(19)

The introduction of electronic apex locators (EALs) into clinical practice has reduced some of the inherent limitations when working length determination solely depended on radiographic information. In 1942, Suzuki discovered the electrical resistance between the periodontal membrane and the oral mucosa to be a constant value of 6.5 kΩ.(20) In 1962, first generation resistance-based EALs were introduced by Sunada.(21) Second generation impedance-based and third generation frequency-based EALs, such as the Root ZX, were subsequently developed.(22, 23)

Apex locators have been found to be accurate to within ±0.5 mm of working length. A popular model is Root ZX (J. Morita, Tokyo, Japan). The accuracy of Root ZX was found to be in the range of 82% to 96%.(24) Welk et al found that the Root ZX accurately located the minor diameter about 90% of the time.(25) Ounsi and Naaman found in an ex vivo study that Root ZX accurately located the apical foramen within ±0.5 mm 84.2% of the time and the apical constriction only 50% of the time; therefore they recommended using the apical foramen, which was marked “Apex” on said device, rather than the apical constriction, which was marked “0.5 mm” for accurate working length determination.(26) However, Shabahang, in an in vivo study, found that Root ZX accurately located to ±0.5 mm the apical foramen 96% of the time using the “0.5” mark instead of the “Apex” mark.(24) Fouad and Krell evaluated five electronic apex locators and found that they were accurate in locating the apical foramen 55-75% of the time to ±0.5 mm and recommended that an adjustment of 0.5 mm from the electronic working length to

be clinically appropriate.(27) Recently, the accuracy of electronic apex locators has been corroborated by studies using cone beam computed tomography. An in-vivo study by Jeger et al found the two modalities to have similar precision with a mean discrepancy of ±0.5 mm.(28) Lucena et al found that measurements by electronic apex locator were more reliable than those by CBCT scan; they found the latter measurements to be 0.59 mm on average shorter than the actual length.(29)

Studies have shown that electronic apex locators perform accurately in the presence of different irrigants,(30, 31) apical root resorption,(32) and in the primary dentition.(33) They have not been found to perform differently in vital versus necrotic cases.(34, 35) In retreatment cases, Mancini found that the presence of gutta percha led to overestimation of working length but Alves found measurement to be accurate after removal of the obturation material.(36, 37) Fuss et al proposed using the electronic apex locator in detection of root perforations.(38)

The importance of early shaping of the cervical root area has been demonstrated in the literature. Stabholz found that coronal flaring significantly improved tactile detection of the apical constriction.(39) Ibarrola found increased efficacy of the apex locator when the coronal canal was flared due to better apical access and patency.(40) De Camargo found that coronal flaring increased the accuracy of working length determination by Root ZX and Mini Apex Locator devices (J. Morita, Tokyo, Japan).(41)

However, few studies have investigated the change in working length after completion of instrumentation. Vasconcelos et al found in their in vitro study that working length was significantly reduced not only after coronal flaring, but also after completion of rotary instrumentation.(42) In their study, the entire instrumentation sequence was performed using a single WaveOne Primary instrument, a reciprocating file system with a variable taper. Only

straight canals (curvature <25°) were studied. The current study was undertaken with a modified study design based on that of Vasconcelos et al to allow for a more traditional instrumentation approach utilizing Gates Glidden drills in coronal flaring and a continuous rotary file system with a constant taper. The effect of canal curvature was also assessed. The aim of this in vitro study was to evaluate the change in working length at various stages of mechanical preparation via direct visualization and electronic apex locator measurements as a function of canal curvature.

Materials and Methods

Forty three extracted mandibular molars were used in this study. Only one mesial canal (mesiobuccal or mesiolingual) from each molar was used, giving a total sample size of 43 canals. Root curvature was measured radiographically using Schneider's technique. In the MiPACS Dental Enterprise Viewer (Medicor Imaging, North Carolina, USA), a straight line was drawn overlapping and paralleling the coronal canal. A second straight line was drawn extending from the apex to the point where the canal started deviating from the coronal root axis. The acute angle formed from the intersection of the two lines was measured using the digital protractor feature, producing the root curvature measurement (see Figure 1). Root curvature was only evaluated from the buccolingual aspect.

Figure 1. Diagrammatic representation of Schneider's method

Coronal standardization was performed with a diamond football bur at high speed to create a flat surface for a reproducible reference point. Access opening was created using #4 round burs and Endo-Z burs at high speed under abundant cooling. The canal was then negotiated with a #10 K-file in the presence of RC-Prep and 0.9% sodium chloride (saline)

irrigation until the file tip was visible through the apical foramen under a dental operating microscope at magnification of 4.65x. This initial working length measurement via direct visualization (DV-unflared) was made with a digital caliper (see Figure 2). The measurement was repeated three times for each tooth.

Figure 2. Measurement with digital caliper

After all direct measurements were recorded, each tooth was mounted in turn for electronic measurement. A Castillo Endo Training Model (VDW, Munich, Germany) was used in conjunction with a CanalPro Apex Locator (Coltène/Whaledent Inc., Ohio, USA). The Endo Training Model is a plastic model of an upper jaw with a socket for mounting of the extracted tooth. The bottom of the socket has a contact pin that connects to the lip clip of the apex locator. The socket was filled with saline and the tooth was mounted with the roots immersed in saline (see Figure 3). The electronic measurements (EM-unflared) were recorded when the device indicated that the file reached the apical foramen (0.0 mm).

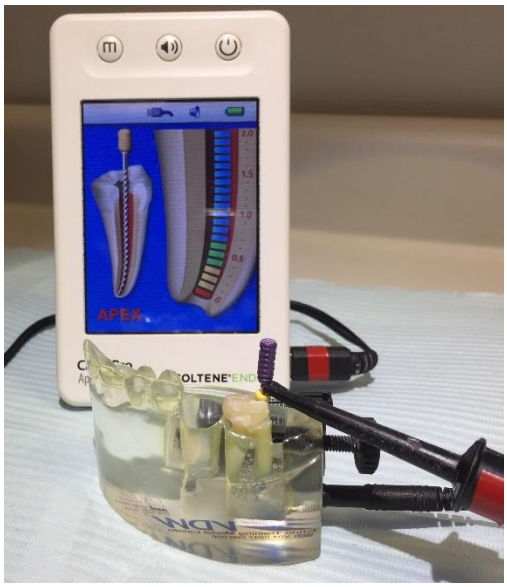

Figure 3. Set up for electronic measurement

Coronal flaring was completed with #2 and #3 Gates Glidden drills on a slow speed hand-piece. Direct measurements (DV-flared) and electronic measurements (EM-flared) were then performed as previously described.

Mechanical instrumentation was completed with .04 taper EndoSequence rotary files operated with an electric motor. A crown-down approach was used until a master apical file size of either #30 or #35 was reached at working length, depending on the degree of root curvature. Direct measurements (DV-concluded) and electronic measurements (EM-concluded) were recorded in the same manner as previously described.

All measurements were performed by a single operator in triplicate with blinding across the time points. Change in working length was assessed using repeated-measures ANCOVA. All analyses were performed using SAS software (JMP Pro version 13.2.1, SAS version 9.4, SAS Institute Inc., Cary NC) at alpha = 0.05 level of significance.

Results

In the results section we first present a description of the teeth included in the study. This is followed by a description of the relationships between working length (WL) and the ΔWL with the unflared (baseline) values and with root curvature. Finally, the multivariable analysis results are presented.

The 43 samples had an average root curvature of 27.69° (SD = 10.00°, range = 9.92° to 50.05°, see Appendix 1: Root Curvature). The average unflared WL as measured by direct visualization (DV) was 18.78 mm (SD = 1.54, range = 14.88 to 21.19) and by electronic measurement (EM) was 18.58 mm (SD = 1.56, range = 14.64 to 22.07, see Appendix 2: Measurements (mm)). The direct visualization measurements were statistically different than the electronic measurements (paired t-test difference = 0.20 mm, SE = 0.037, $P < .0001$). This is seen in Figure 4 where, in the pair of DV and EM measurements, the DV values are slightly larger. The correlation between curvature and unflared working length is also evident (Pearson's $r = –0.30$, $P < .0001$). In other words, among the roots selected for this study, the shorter roots tended to have greater curvatures and the longer roots tended to have less curvatures.

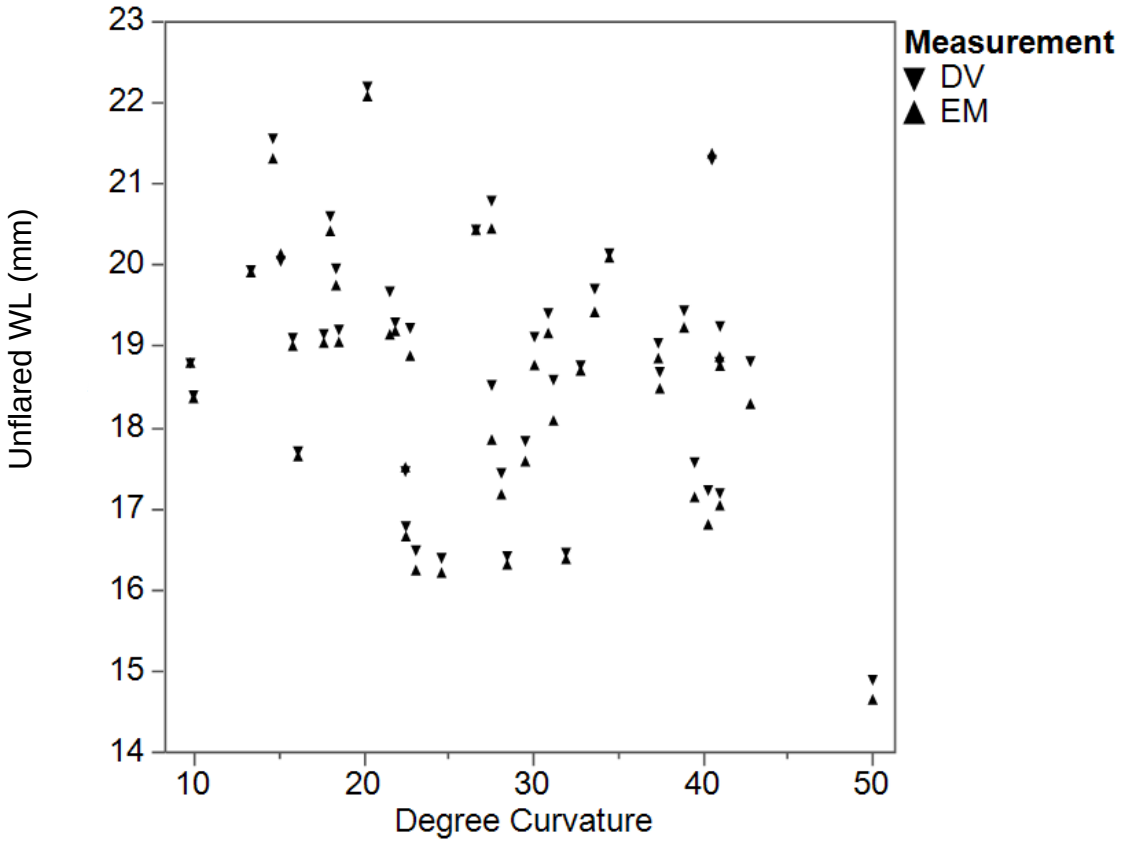

Figure 4. Relationship between unflared working length and root curvature

The primary aim of this study was to describe the change in WL between the three time points: Unflared, Flared, and Concluded as measured by direct visualization (DV) and electronic measurement (EM). The average unflared WL of each root was taken as the baseline. As Figure 5 shows, WL (y-axis) at each time point is strongly related to the baseline WL (x-axis).

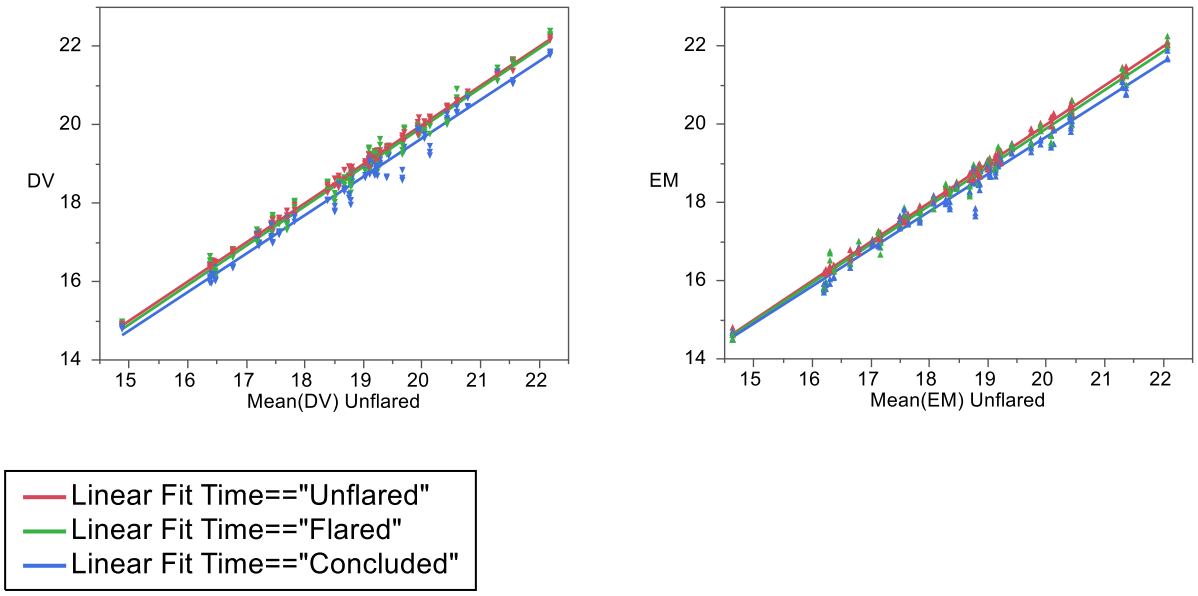

Figure 5. DV and EM working length measurements as a function of the baseline (unflared) working length.

The change in working length as measured by direct visualization can be represented by the following equation: $\Delta DV_{i,t,r} = DV_{i,t,r} - \overline{DV}_{i,unflared}$. Since each measurement was repeated 3 times, each replicate was represented by *r* (*r* = 1 to 3). The time point is represented by *t* (*t* = unflared, flared, concluded). Each root was indexed as *i* (*i* = 1 to 43). The changes in working length as determined by direct visualization and electronic measurement are represented by the ΔDV and the ΔEM respectively. The mean of the three replicates of unflared DV measurements for root *i* is presented as $\overline{DV}_{i,unflared}$. Similarly, the change in working length determined by electronic measurement is represented as: $\Delta EM_{i,t,r} = EM_{i,t,r} - \overline{EM}_{i,unflared}$.

Although the change in WL is somewhat evident in Figure 5, it is shown directly in Figure 6. On the left panel we see the relationship between the $\Delta DV_{i,t,r}$ and $\overline{DV}_{i,unflared}$. The red line shows the relationship between each unflared measurement and that root's average unflared

measurement and is thus a flat line at zero (no change). The green line shows the relationship between the ΔDV_{flared} (y-axis) and mean $DV_{unflared}$ (x-axis). On average, DV_{flared} appears to be approximately 0.1 shorter than mean $DV_{unflared}$, and a slightly smaller change in WL (ΔDV_{flared}) was observed in longer roots than in shorter roots. This contrasts with the right-hand panel of Figure 6, which shows that a greater ΔEM_{flared} was observed in longer roots than in shorter roots. The blue lines show the $\Delta DV_{concluded}$ and the $\Delta EM_{concluded}$ values as a function of mean $DV_{unflared}$ and mean $EM_{unflared}$ respectively. There appears to be less of a trend for the $\Delta DV_{concluded}$ than for the $\Delta EM_{concluded}$; i.e., there was a greater $\Delta EM_{concluded}$ in longer roots than in shorter roots. This trend was less obvious for the $\Delta DV_{concluded}$ (steeper slope of blue line for the $\Delta EM_{concluded}$ compared with the $\Delta DV_{concluded}$).

These descriptions are meant to illustrate the following observations: (1) there appears to be a relationship between the ΔWL values and root length, (2) the ΔWL values appear to be different depending upon the measurement technique (DV vs EM), and (3) the relationship (trend) with root length may be different for DV and EM across time points.

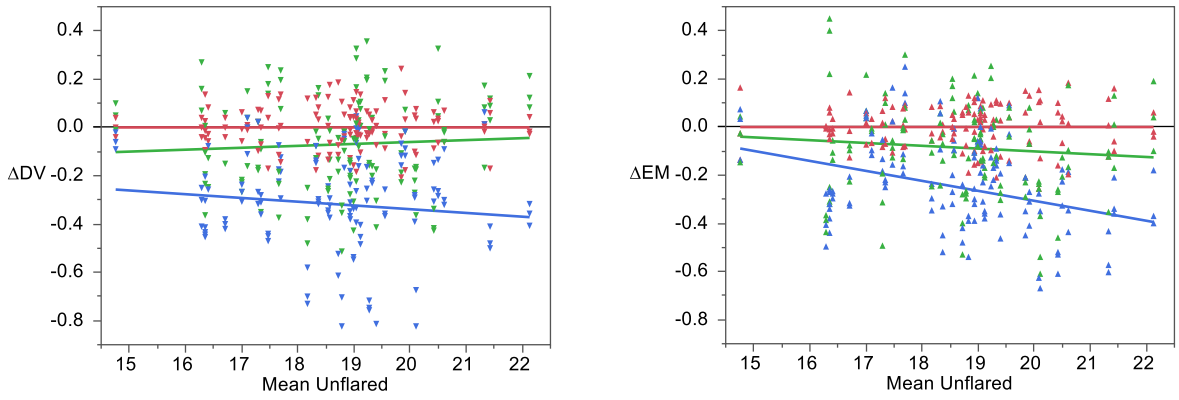

Figure 6. ΔDV and ΔEM working length measurements as a function of the baseline (unflared) working length

Regarding the relationship between the ΔWL and root curvature, Figure 7 shows the relationship between the $\Delta DV_{i,t,r}$ and $Curvature_i$ on the left, and the $\Delta EM_{i,t,r}$ and $Curvature_i$ on the right. As previously presented, the red line indicates no change between unflared and unflared, the green line indicates change between flared and unflared, and the blue line indicates change between concluded and unflared. A smaller ΔDV_{flared} (green line) was observed in straighter roots than in curved roots, but the opposite trend was observed with the ΔEM_{flared}. For both $\Delta DV_{concluded}$ and $\Delta EM_{concluded}$ (blue lines), there was a greater change in WL with straight roots than curved roots. This trend was slightly more pronounced for the $\Delta EM_{concluded}$ than the $\Delta DV_{concluded}$ (steeper slope of blue line for the $\Delta EM_{concluded}$ than the $\Delta DV_{concluded}$). Just as previously discussed with respect to root length, the following three observations are made regarding root curvature: (1) there appears to be a relationship between the ΔWL values and curvature, (2) the ΔWL values appear to be different depending upon the measurement technique

(DV vs EM), and (3) the relationship (trend) with curvature may be different for DV and EM across time points.

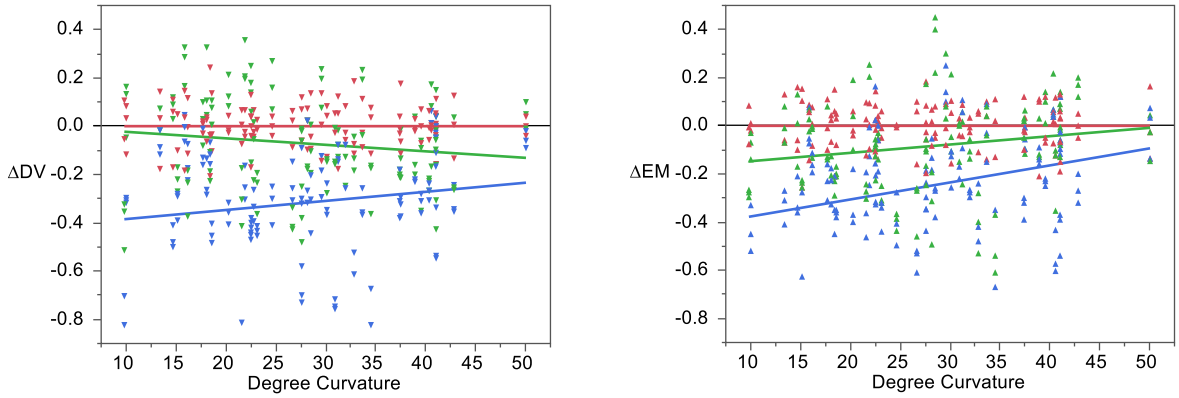

Figure 7. ΔDV and ΔEM working length measurements as a function of root curvature

These results motivate the choice of factors to include in the final analysis model of the ΔWL. The analysis model used was a repeated-measures ANCOVA, where the trends observed (above) indicated the need for the following covariates: (baseline) Unflared WL and Degree Curvature. The other factors included in the model are: Technique (DV vs EM), Time (flared vs concluded), the Technique*Time interaction, and the interactions that permit the covariate trends to be different depending upon Technique and Time. A mixed-model repeated-measurements ANCOVA was used to account for the correlations among all of the measurements on each root.

The analysis indicated that, after taking all of the factors into account, the difference between the ΔDV and the ΔEM varied depending upon the measurement time point (P = 0.0043). This is shown in the estimated ΔWL values in Table 1. For the average canal length (average unflared length = 18.68 mm) and the average curvature = 27.69°), an average ΔDV_{flared} of approximately –0.07 mm and average ΔEM_{flared} of approximately –0.09 mm, were found, which

are not significantly different (P > 0.3). However, for the average root after conclusion of instrumentation, the average $\Delta DV_{concluded}$ is –0.31 mm and the average $\Delta EM_{concluded}$ is –0.26 mm, which are statistically different (P = 0.003).

Table 1. Overall ΔWL depending upon Time and Technique

Time	Technique	ΔWL (mm)	95% CI		P-value*
Flared	DV	-0.0688	-0.1196	-0.0179	0.3298
	EM	-0.0878	-0.1387	-0.0370	
Concluded	DV	-0.3139	-0.3648	-0.2631	0.0030
	EM	-0.2556	-0.3065	-0.2047	

Abbreviations: DV=direct visualization, EM=electronic measurement, ΔWL=estimated average change in working length as compared to the average unflared measurement, 95% CI=95% confidence interval

*P-values, estimates, and confidence intervals estimated from a repeated-measures mixed model ANCOVA. The estimates are for the average unflared root length (18.68 mm) and the average curvature (27.69°). The P-value compares the DV and EM estimate at the specified Time.

The analysis also indicated the difference between the ΔDV and the ΔEM does not depend upon the unflared working length of the root. These estimates and their 95% confidence intervals are shown in Table 2. Note that at the flared stage, for all unflared working lengths, there is no statistically significant difference between the ΔDV and the ΔEM (P = 0.3298) but there is a difference at conclusion of instrumentation, with a greater change being measured via direct visualization (P = 0.0030). This is demonstrated graphically in Figure 8; there is little vertical separation between the DV and EM lines in the top graph (flared stage), but there is a greater vertical separation in the bottom graph (at conclusion). The parallel lines in Figure 8 indicate that the relationship (trend) between the ΔWL and unflared WL is the same for DV and EM. In other words, the change in working length depends on the baseline unflared working length, and this relationship is the same for DV and EM.

Table 2. ΔWL depending upon Unflared Working Length, Time and Technique

Unflared WL	Time	Measurement	ΔWL (mm)	95% CI		P-value*
15	Flared	DV	0.0107	-0.1199	0.1414	0.3298
		EM	-0.0083	-0.1331	0.1165	
	Concluded	DV	-0.1620	-0.2926	-0.0313	0.0030
		EM	-0.1036	-0.2285	0.0212	
16	Flared	DV	-0.0109	-0.1129	0.0911	0.3298
		EM	-0.0299	-0.1265	0.0666	
	Concluded	DV	-0.2033	-0.3053	-0.1013	0.0030
		EM	-0.1450	-0.2415	-0.0484	
17	Flared	DV	-0.0325	-0.1086	0.0435	0.3298
		EM	-0.0516	-0.1230	0.0199	
	Concluded	DV	-0.2447	-0.3207	-0.1686	0.0030
		EM	-0.1863	-0.2578	-0.1149	
18	Flared	DV	-0.0542	-0.1106	0.0023	0.3298
		EM	-0.0732	-0.1272	-0.0192	
	Concluded	DV	-0.2860	-0.3425	-0.2295	0.0030
		EM	-0.2277	-0.2817	-0.1737	
19	Flared	DV	-0.0758	-0.1271	-0.0245	0.3298
		EM	-0.0948	-0.1474	-0.0423	
	Concluded	DV	-0.3274	-0.3786	-0.2761	0.0030
		EM	-0.2690	-0.3216	-0.2165	
20	Flared	DV	-0.0974	-0.1615	-0.0334	0.3298
		EM	-0.1165	-0.1846	-0.0484	
	Concluded	DV	-0.3687	-0.4327	-0.3047	0.0030
		EM	-0.3104	-0.3785	-0.2423	
21	Flared	DV	-0.1191	-0.2063	-0.0318	0.3298
		EM	-0.1381	-0.2306	-0.0456	
	Concluded	DV	-0.4100	-0.4973	-0.3228	0.0030
		EM	-0.3517	-0.4442	-0.2592	
22	Flared	DV	-0.1407	-0.2554	-0.0260	0.3298
		EM	-0.1597	-0.2802	-0.0393	
	Concluded	DV	-0.4514	-0.5661	-0.3367	0.0030
		EM	-0.3931	-0.5135	-0.2726	

Abbreviations: DV=direct visualization, EM=electronic measurement, ΔWL=estimated average change in working length as compared to the average unflared measurement, 95% CI=95% confidence interval

*P-values, estimates, and confidence intervals estimated from a repeated-measures mixed model ANCOVA. The estimates are for the average curvature (28°) The P-value compares the DV and EM estimate at the specified Unflared Working Length and Time.

Flared

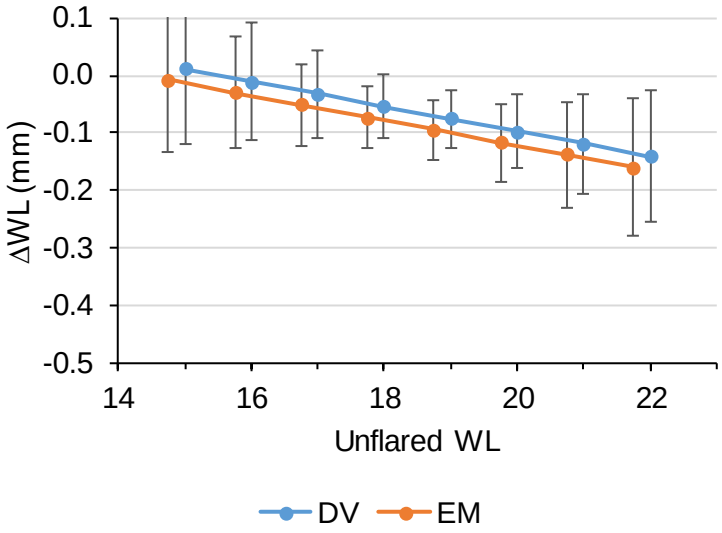

Concluded

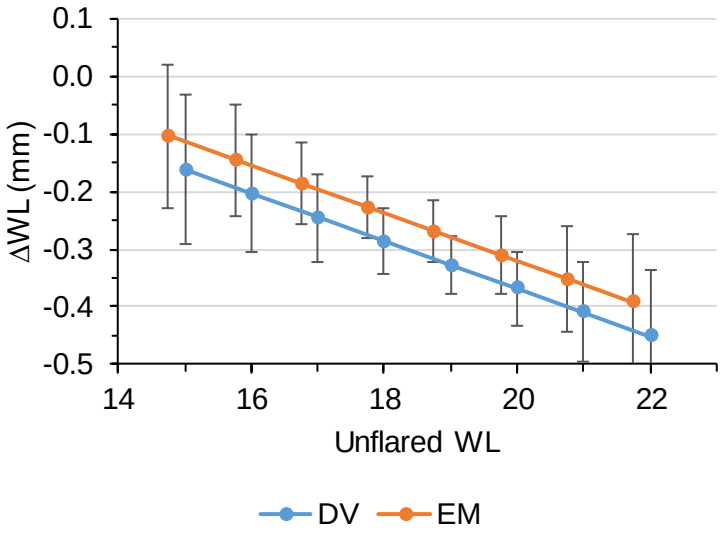

Figure 8. ΔWL depending upon Unflared Working Length and Technique for the Flared (top panel) and Concluded (bottom panel) time points

However, the difference between the ΔDV and the ΔEM depends upon root curvature (P = 0.0010). This is shown in Table 3. For roots with curvature < 25°, a significant difference between the ΔDV_{flared} and the ΔEM_{flared} was found at the flared stage, but not at conclusion. In contrast, roots with curvatures > 25°, a significant difference between the $\Delta DV_{concluded}$ and the $\Delta EM_{concluded}$ was found at conclusion, but not at the flared stage. These estimates and their 95% confidence intervals are shown in Table 3. Figure 9 shows the trend between root curvature and the ΔWL at the flared and concluded time points for DV and EM. In the top panel, a downward trend of the blue (ΔDV) line is demonstrated, indicating that as curvature increases, the ΔDV_{flared} increases; the upward trend of the orange (ΔEM) line indicates that as curvature increases, the ΔEM_{flared} decreases. In the bottom panel, the generally flat blue line indicates that curvature has very little relationship to the $\Delta DV_{concluded}$. However, the upward trending orange line indicates that as curvature increases, the $\Delta EM_{concluded}$ decreases.

Table 3. ΔWL depending upon Curvature, Time and Technique

Curvature	Time	Technique	ΔWL (mm)	95% CI		P-value*
15	Flared	DV	-0.0321	-0.1154	0.0512	0.0034
		EM	-0.1089	-0.1913	-0.0266	
	Concluded	DV	-0.3296	-0.4129	-0.2463	0.9833
		EM	-0.3291	-0.4114	-0.2467	
20	Flared	DV	-0.0466	-0.1115	0.0184	0.0149
		EM	-0.1006	-0.1646	-0.0366	
	Concluded	DV	-0.3234	-0.3883	-0.2585	0.2926
		EM	-0.3001	-0.3641	-0.2361	
25	Flared	DV	-0.0610	-0.1139	-0.0081	0.1153
		EM	-0.0923	-0.1448	-0.0398	
	Concluded	DV	-0.3173	-0.3702	-0.2643	0.0207
		EM	-0.2712	-0.3237	-0.2187	
30	Flared	DV	-0.0754	-0.1275	-0.0234	0.6665
		EM	-0.0840	-0.1364	-0.0315	
	Concluded	DV	-0.3111	-0.3631	-0.2590	0.0006
		EM	-0.2422	-0.2947	-0.1898	
35	Flared	DV	-0.0899	-0.1526	-0.0272	0.5193
		EM	-0.0757	-0.1396	-0.0117	
	Concluded	DV	-0.3049	-0.3676	-0.2422	<.0001
		EM	-0.2133	-0.2773	-0.1493	
40	Flared	DV	-0.1043	-0.1847	-0.0239	0.1550
		EM	-0.0673	-0.1496	0.0150	
	Concluded	DV	-0.2987	-0.3791	-0.2183	<.0001
		EM	-0.1844	-0.2667	-0.1021	
45	Flared	DV	-0.1188	-0.2204	-0.0172	0.0540
		EM	-0.0590	-0.1629	0.0449	
	Concluded	DV	-0.2925	-0.3942	-0.1909	<.0001
		EM	-0.1554	-0.2593	-0.0515	

Abbreviations: DV=direct visualization, EM=electronic measurement, ΔWL=estimated average change in working length as compared to the average unflared measurement, 95% CI=95% confidence interval

*P-values, estimates, and confidence intervals estimated from a repeated-measures mixed model ANCOVA. The estimates are for the average unflared root length (18.68 mm) The P-value compares the DV and EM estimate at the specified Curvature and Time.

Flared

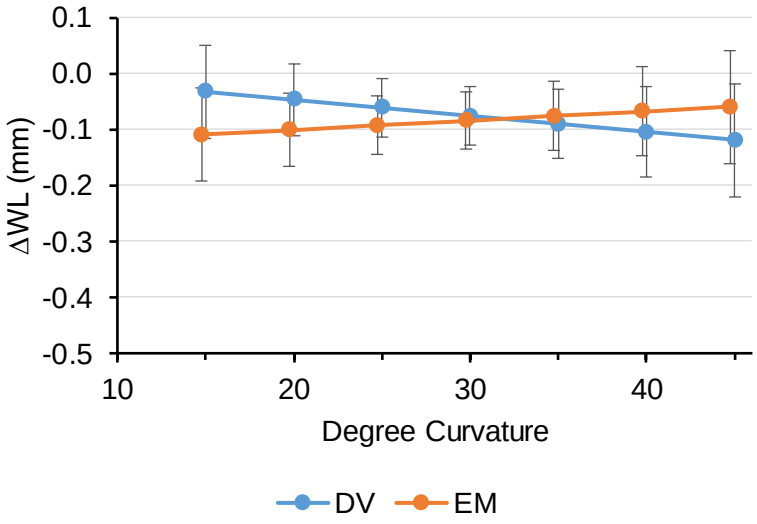

Concluded

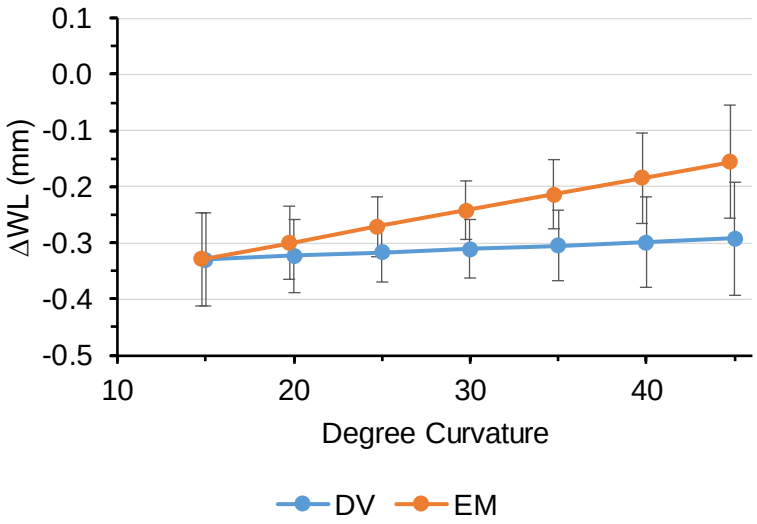

Figure 9. ΔWL depending upon Curvature and Technique for the Flared (top panel) and Concluded (bottom panel) time points

Discussion

This study was undertaken to investigate the change in working length across various time points of mechanical preparation, namely the unflared-flared stage and the unflared-concluded stage. Working lengths were measured by direct visualization and electronically. The effect of canal curvature was evaluated.

One mesial canal of each of 43 extracted mandibular molars was used in the study. This way, teeth with joining MB and ML canals could be used without interference of the other canal. Canal curvature was measured radiographically using Schneider's technique. One limitation of this study was that the curvature was only evaluated from the buccolingual aspect. Hence, only the mesiodistal canal curvature was accounted for. Canals that appeared to be straight might in fact have an unknown amount of buccolingual curvature.

Each working length measurement was repeated three times with both measurement techniques. That means the measuring file was completely removed before re-insertion into the canal for each subsequent measurement. With direct visualization, one challenge was to select a reference point at which the file tip was considered visible through the apical foramen. The apical foramen is not a perfectly regular shape, and dentin debris accompanying the file tip can make visualization difficult. Each successive measurement also resulted in removal of apical tooth structure. In addition, the blinding of the operator across time points could have resulted in a slightly different reference point being selected at subsequent stages of mechanical preparation. All these factors of human error may have contributed to the statistically larger DV measurements compared to the EM measurements (paired t-test difference = 0.20 mm).

This study found a change of working length of –0.07 mm by direct visualization and –0.09 mm by electronic measurement from the unflared to flared time points. The difference

between the two measurement techniques was not statistically significant ($P > 0.3$). At the unflared to concluded time points, changes of –0.31 mm and –0.26 mm were found by direct visualization and electronic measurement respectively, with a statistically significant difference between the two values ($P = 0.003$). Clinically, a 0.5 mm difference in working length is discernible visually. However, it may be much more difficult to consistently discern a 0.25 mm difference. Therefore, even though an overall loss of working length (unflared-concluded) of 0.26 mm and 0.31 mm was found in this study by electronic measurement and direct visualization respectively, a limited degree of clinical significance may be extrapolated.

The statistical analysis model ANCOVA, taking into account the factors of baseline working lengths, curvatures, measurement techniques and time points, revealed that overall, a greater change in working length was observed in longer roots than in shorter roots. The greater the canal curvature, the smaller the change in working length was observed. The largest change in working length was observed in straight canals. Canals with curvature < 25° showed a loss in working length greater than 0.25 mm measured by both direct visualization and electronic measurement. This finding is counter-intuitive as one would expect a canal with greater curvature to undergo greater canal straightening and therefore greater loss of working length compared with a straight canal. This unexpected finding may be attributed to three limitations of this study. First, canal curvature was evaluated radiographically only in one dimension. Second, the sample size was limited and there was relationship between root length and root curvature in this sample, where longer canals tended to be straighter and shorter canals tended to be more curved. As previously mentioned, a greater change in working length was found in longer canals, which tended to be straighter. Therefore, the canal curvature and length relationship may be a confounding factor. Third, the effect of master apical file size was not taken into account in the

study design and was not standardized for curvature or recorded for retrospective analysis. It is possible that a larger master apical file size was achieved in straighter canals and larger files tend to cause greater canal straightening. However, one limitation in the study design was the lack of standardization of master apical size with canal curvature, and the MAF size was not recorded for retrospective analysis.

In this study, a smaller change in working length was found, compared to the study by Vasconcelos et al. They found an average reduction of working length after flaring to be 0.34 mm, and a 0.6 mm overall reduction was observed at the conclusion of instrumentation. They also found a reduction in working length up to 1.75 mm in some canals and attributed this to the removal of cervical deposition of secondary dentin.(42) In our study, the amount of working length reduction was less than 0.10 mm after flaring and 0.3 mm after completion of instrumentation. This discrepancy may be attributed to the differences in study design. In the study by Vasconcelos et al, only canals with curvature < 25° were studied. A single WaveOne Primary instrument was used for cervical flaring as well as complete instrumentation. This is an instrument with a tip size of ISO #25 and an .08 apical taper that reduces towards the coronal end. In our study, cervical flaring was achieved by #2 and #3 Gates Glidden drills and complete instrumentation was performed with .04 taper EndoSequence files up to a size #30 or #35. It is possible that the smaller taper instruments may have resulted in less canal straightening.

Conclusion

In this study, a greater change in working length was observed in straight canals than in curved canals. This unexpected finding was attributed to the limitations of the study, specifically the confounding factor of root length. This trend was more pronounced when measured electronically than via direct visualization, especially after complete instrumentation than after coronal flaring. The overall change in working length after complete instrumentation was found to be clinically insignificant in this study. A limited amount of change in working length may be expected prior to obturation.

References

1. Davis MS, Joseph SW, Bucher JF. Periapical and intracanal healing following incomplete root canal fillings in dogs. Oral Surgery, Oral Medicine, Oral Pathology. 1971;31(5):662-75.

2. Swartz DB, Skidmore AE, Griffin JA. Twenty years of endodontic success and failure. Journal of Endodontics. 1983;9(5):198-202.

3. Ricucci D. Apical limit of root canal instrumentation and obturation, part 1. literature review. International Endodontic Journal. 1998;31(6):384-93.

4. Ng Y, Mann V, Rahbaran S, Lewsey J, Gulabivala K. Outcome of primary root canal treatment: Systematic review of the literature–Part 2. influence of clinical factors. International Endodontic Journal. 2008;41(1):6-31.

5. Sjögren U, Figdor D, Persson S, Sundqvist G. Influence of infection at the time of root filling on the outcome of endodontic treatment of teeth with apical periodontitis. International Endodontic Journal. 1997;30(5):297-306.

6. Kuttler Y. Microscopic investigation of root apexes. Journal of the American Dental Association. 1955;50(5):544-52.

7. Green D. Stereomicroscopic study of 700 root apices of maxillary and mandibular posterior teeth. Oral Surgery, Oral Medicine, Oral Pathology. 1960;13(6):728-33.

8. Burch JG, Hulen S. The relationship of the apical foramen to the anatomic apex of the tooth root. Oral Surgery, Oral Medicine, Oral Pathology. 1972;34(2):262-8.

9. ElAyouti A, Hülber-J M, Judenhofer MS, Connert T, Mannheim JG, Löst C, et al. Apical constriction: Location and dimensions in molars—a micro–computed tomography study. Journal of Endodontics. 2014;40(8):1095-9.

10. Coolidge ED. Anatomy of the root apex in relation to treatment problems. Journal of the American Dental Association. 1922. 1929;16(8):1456-65.

11. Orban B. Why root canals should be filled to the dentinocemental junction. Journal of the American Dental Association. 1930;17(6):1086-7.

12. Meder-Cowherd L, Williamson AE, Johnson WT, Vasilescu D, Walton R, Qian F. Apical morphology of the palatal roots of maxillary molars by using micro–computed tomography. Journal of Endodontics. 2011;37(8):1162-5.

13. Voorde HV, Bjorndahl AM. Estimating endodontic "working length" with paralleling radiographs. Oral Surgery, Oral Medicine, Oral Pathology. 1969;27(1):106-10.

14. Olson A, Goering A, Cavataio R, Luciano J. The ability of the radiograph to determine the location of the apical foramen. International Endodontic Journal. 1991;24(1):28-35.

15. Tamse A, Kaffe I, Fishel D. Zygomatic arch interference with correct radiographic diagnosis in maxillary molar endodontics. Oral Surgery, Oral Medicine, Oral Pathology. 1980;50(6):563-5.

16. Green D. A stereo-binocular microscopic study of the root apices and surrounding areas of 100 mandibular molars: Preliminary study. Oral Surgery, Oral Medicine, Oral Pathology. 1955;8(12):1298-304.

17. Williams CB, Joyce AP, Roberts S. A comparison between in vivo radiographic working length determination and measurement after extraction. Journal of Endodontics. 2006 7;32(7):624-7.

18. Stein TJ, Corcoran JF. Radiographic "working length" revisited. Oral Surgery, Oral Medicine, Oral Pathology. 1992;74(6):796-800.

19. ElAyouti A, Weiger R, Löst C. Frequency of overinstrumentation with an acceptable radiographic working length. Journal of Endodontics. 2001;27(1):49-52.

20. Suzuki K. Experimental study on iontophoresis. Journal of the Japanese Stomatological Society. 1942;16:411.

21. Sunada I. New method for measuring the length of the root canal. Journal of Dental Research. 1962;41(2):375-87.

22. Kobayashi C, Suda H. New electronic canal measuring device based on the ratio method. Journal of Endodontics. 1994;20(3):111-4.

23. Kobayashi C. Electronic canal length measurement. Oral Surgery, Oral Medicine, Oral Pathology, Oral Radiology, and Endodontology. 1995;79(2):226-31.

24. Shabahang S, Goon WW, Gluskin AH. An in vivo evaluation of root ZX electronic apex locator. Journal of Endodontics. 1996;22(11):616-8.

25. Welk AR, Baumgartner JC, Marshall JG. An in vivo comparison of two frequency-based electronic apex locators. Journal of Endodontics. 2003;29(8):497-500.

26. Ounsi H, Naaman A. In vitro evaluation of the reliability of the root ZX electronic apex locator. International Endodontic Journal. 1999;32(2):120-3.

27. Fouad AF, Krell KV, McKendry DJ, Koorbusch GF, Olson RA. A clinical evaluation of five electronic root canal length measuring instruments. Journal of Endodontics. 1990;16(9):446-9.

28. Jeger FB, Janner SF, Bornstein MM, Lussi A. Endodontic working length measurement with preexisting cone-beam computed tomography scanning: A prospective, controlled clinical study. Journal of Endodontics. 2012;38(7):884-8.

29. Lucena C, López J, Martín J, Robles V, González-Rodríguez M. Accuracy of working length measurement: Electronic apex locator versus cone-beam computed tomography. International Endodontic Journal. 2014;47(3):246-56.

30. Jenkins JA, Walker WA, Schindler WG, Flores CM. An in vitro evaluation of the accuracy of the root ZX in the presence of various irrigants. Journal of Endodontics. 2001;27(3):209-11.

31. Meares WA, Steiman HR. The influence of sodium hypochlorite irrigation on the accuracy of the root ZX electronic apex locator. Journal of Endodontics. 2002;28(8):595-8.

32. Goldberg F, De Silvio AC, Manfré S, Nastri N. In vitro measurement accuracy of an electronic apex locator in teeth with simulated apical root resorption. Journal of Endodontics. 2002;28(6):461-3.

33. Katz A, Mass E, Kaufman AY. Electronic apex locator: A useful tool for root canal treatment in the primary dentition. ASDC Journal of Dentistry for Children. 1996 Nov-Dec;63(6):414-7.

34. Dunlap CA, Remeikis NA, BeGole EA, Rauschenberger CR. An in vivo evaluation of an electronic apex locator that uses the ratio method in vital and necrotic canals. Journal of Endodontics. 1998;24(1):48-50.

35. Akisue E, Gavini G, de Figueiredo, Jose Antonio Poli. Influence of pulp vitality on length determination by using the elements diagnostic unit and apex locator. Oral Surgery, Oral Medicine, Oral Pathology, Oral Radiology, and Endodontology. 2007;104(4):e129-32.

36. Mancini M, Palopoli P, Iorio L, Conte G, Cianconi L. Accuracy of an electronic apex locator in the retreatment of teeth obturated with plastic or cross-linked gutta-percha carrier-based materials: An ex vivo study. Journal of Endodontics. 2014;40(12):2061-5.

37. Alves A, Felippe M, Felippe W, Rocha M. Ex vivo evaluation of the capacity of the tri auto ZX to locate the apical foramen during root canal retreatment. International Endodontic Journal. 2005;38(10):718-24.

38. Fuss Z, Assooline LS, Kaufman AY. Determination of location of root perforations by electronic apex locators. Oral Surgery, Oral Medicine, Oral Pathology, Oral Radiology, and Endodontology. 1996;82(3):324-9.

39. Stabholz A, Rotstein I, Torabinejad M. Effect of preflaring on tactile detection of the apical constriction. Journal of Endodontics. 1995 Feb;21(2):92-4.

40. Ibarrola JL, Chapman BL, Howard JH, Knowles KI, Ludlow MO. Effect of preflaring on root ZX apex locators. Journal of Endodontics. 1999;25(9):625-6.

41. de Camargo ÉJ, Zapata RO, Medeiros PL, Bramante CM, Bernardineli N, Garcia RB, et al. Influence of preflaring on the accuracy of length determination with four electronic apex locators. Journal of Endodontics. 2009;35(9):1300-2.

42. Vasconcelos BC, Bastos LM, Oliveira AS, Bernardes RA, Duarte MA, Vivacqua-Gomes N, et al. Changes in root canal length determined during mechanical preparation stages and their relationship with the accuracy of root ZX II. Journal of Endodontics. 2016 Nov;42(11):1683-6.

Appendices

Appendix 1: Root Curvature

Tooth	Degree Curvature
C-1	31.97
C-2	40.57
C-3	26.66
C-6	37.41
C-7	50.05
C-8	41.04
C-9	37.50
C-10	33.66
C-11	40.35
C-12	38.93
C-13	41.02
C-14	42.84
C-15	29.57
C-16	31.23
C-17	34.52
C-18	32.83
C-19	27.59
C-20	39.55
C-21	41.05
C-22	30.11
S-1	15.15
S-2	13.39
S-3	16.17
S-4	27.58
S-5	30.92
S-6	18.58
S-7	18.41
S-8	14.69
S-9	20.26
S-10	21.90
S-11	10.01
S-12	15.86
S-13	22.78
S-14	24.63
S-15	28.16
S-16	9.82
S-17	17.69
S-18	18.07

Tooth	Degree Curvature
S-19	21.58
S-20	28.50
S-21	22.50
S-22	23.12
S-24	22.53

Appendix 2: Measurements (mm)

Tooth	Time	Rep	DV	EM
C-1	Unflared	1	16.42	16.34
C-1	Unflared	2	16.53	16.36
C-1	Unflared	3	16.39	16.40
C-1	Flared	1	16.20	16.23
C-1	Flared	2	16.32	16.31
C-1	Flared	3	16.32	16.26
C-1	Concluded	1	16.19	16.09
C-1	Concluded	2	16.37	16.10
C-1	Concluded	3	16.37	16.07
C-2	Unflared	1	21.30	21.24
C-2	Unflared	2	21.27	21.37
C-2	Unflared	3	21.29	21.48
C-2	Flared	1	21.12	21.26
C-2	Flared	2	21.37	21.24
C-2	Flared	3	21.46	21.01
C-2	Concluded	1	21.35	20.79
C-2	Concluded	2	21.35	20.93
C-2	Concluded	3	21.30	20.76
C-3	Unflared	1	20.45	20.26
C-3	Unflared	2	20.49	20.52
C-3	Unflared	3	20.34	20.48
C-3	Flared	1	20.01	20.16
C-3	Flared	2	20.09	20.15
C-3	Flared	3	20.00	19.96
C-3	Concluded	1	20.17	19.81
C-3	Concluded	2	20.28	19.89
C-3	Concluded	3	20.12	19.90
C-6	Unflared	1	19.00	18.82
C-6	Unflared	2	19.07	18.74
C-6	Unflared	3	19.02	18.96
C-6	Flared	1	18.82	18.87
C-6	Flared	2	18.85	18.79
C-6	Flared	3	18.83	18.86
C-6	Concluded	1	18.65	18.52
C-6	Concluded	2	18.85	18.54
C-6	Concluded	3	18.72	18.45
C-7	Unflared	1	14.92	14.50
C-7	Unflared	2	14.84	14.61
C-7	Unflared	3	14.88	14.80
C-7	Flared	1	14.87	14.49
C-7	Flared	2	14.98	14.68
C-7	Flared	3	14.93	14.61
C-7	Concluded	1	14.86	14.67
C-7	Concluded	2	14.79	14.50
C-7	Concluded	3	14.82	14.71
C-8	Unflared	1	17.18	17.06
C-8	Unflared	2	17.19	16.96
C-8	Unflared	3	17.17	17.06
C-8	Flared	1	17.02	17.01
C-8	Flared	2	17.33	17.02
C-8	Flared	3	17.22	17.01
C-8	Concluded	1	17.18	16.93
C-8	Concluded	2	17.07	16.91
C-8	Concluded	3	17.22	17.00
C-9	Unflared	1	18.85	18.44
C-9	Unflared	2	18.61	18.50
C-9	Unflared	3	18.56	18.46
C-9	Flared	1	18.46	18.35
C-9	Flared	2	18.54	18.53
C-9	Flared	3	18.66	18.37
C-9	Concluded	1	18.30	18.37
C-9	Concluded	2	18.35	18.41
C-9	Concluded	3	18.38	18.46
C-10	Unflared	1	19.67	19.27
C-10	Unflared	2	19.81	19.45
C-10	Unflared	3	19.61	19.51
C-10	Flared	1	19.89	19.45
C-10	Flared	2	19.93	19.49

Tooth	Time	Rep	DV	EM
C-10	Flared	3	19.66	19.37
C-10	Concluded	1	19.33	19.26
C-10	Concluded	2	19.34	19.38
C-10	Concluded	3	19.44	19.50
C-11	Unflared	1	17.21	16.81
C-11	Unflared	2	17.16	16.85
C-11	Unflared	3	17.28	16.72
C-11	Flared	1	17.00	16.83
C-11	Flared	2	16.95	17.01
C-11	Flared	3	16.99	16.86
C-11	Concluded	1	16.91	16.84
C-11	Concluded	2	16.95	16.86
C-11	Concluded	3	16.98	16.83
C-12	Unflared	1	19.42	19.01
C-12	Unflared	2	19.41	19.32
C-12	Unflared	3	19.46	19.33
C-12	Flared	1	19.23	19.09
C-12	Flared	2	19.27	19.10
C-12	Flared	3	19.47	19.25
C-12	Concluded	1	19.20	19.13
C-12	Concluded	2	19.21	19.06
C-12	Concluded	3	19.20	19.08
C-13	Unflared	1	18.85	18.99
C-13	Unflared	2	18.76	18.67
C-13	Unflared	3	18.78	18.92
C-13	Flared	1	18.74	18.93
C-13	Flared	2	18.78	18.95
C-13	Flared	3	18.70	18.73
C-13	Concluded	1	18.75	18.49
C-13	Concluded	2	18.63	18.32
C-13	Concluded	3	18.77	18.47
C-14	Unflared	1	18.81	18.23
C-14	Unflared	2	18.93	18.28
C-14	Unflared	3	18.67	18.33
C-14	Flared	1	18.54	18.45
C-14	Flared	2	18.84	18.48
C-14	Flared	3	18.55	18.40
C-14	Concluded	1	18.56	18.01
C-14	Concluded	2	18.45	18.08
C-14	Concluded	3	18.46	17.96
C-15	Unflared	1	17.83	17.49
C-15	Unflared	2	17.96	17.56
C-15	Unflared	3	17.68	17.66
C-15	Flared	1	17.90	17.87
C-15	Flared	2	18.06	17.60
C-15	Flared	3	18.02	17.65
C-15	Concluded	1	17.53	17.71
C-15	Concluded	2	17.64	17.67
C-15	Concluded	3	17.70	17.82
C-16	Unflared	1	18.63	18.03
C-16	Unflared	2	18.40	18.03
C-16	Unflared	3	18.70	18.16
C-16	Flared	1	18.50	17.83
C-16	Flared	2	18.56	18.13
C-16	Flared	3	18.45	18.09
C-16	Concluded	1	18.43	18.13
C-16	Concluded	2	18.50	17.98
C-16	Concluded	3	18.44	18.18
C-17	Unflared	1	20.02	19.95
C-17	Unflared	2	20.17	20.19
C-17	Unflared	3	20.21	20.10
C-17	Flared	1	19.96	19.47
C-17	Flared	2	19.97	19.54
C-17	Flared	3	19.77	19.71
C-17	Concluded	1	19.46	19.41
C-17	Concluded	2	19.22	19.41
C-17	Concluded	3	19.31	19.73
C-18	Unflared	1	18.68	18.75
C-18	Unflared	2	18.64	18.58
C-18	Unflared	3	18.94	18.74
C-18	Flared	1	18.62	18.16
C-18	Flared	2	18.57	18.29
C-18	Flared	3	18.71	18.41
C-18	Concluded	1	18.14	18.21
C-18	Concluded	2	18.23	18.27
C-18	Concluded	3	18.23	18.45
C-19	Unflared	1	18.63	17.78
C-19	Unflared	2	18.45	17.92
C-19	Unflared	3	18.45	17.81
C-19	Flared	1	18.26	17.78
C-19	Flared	2	18.13	17.73
C-19	Flared	3	18.03	17.59
C-19	Concluded	1	17.93	17.54
C-19	Concluded	2	17.78	17.60
C-19	Concluded	3	17.81	17.49
C-20	Unflared	1	17.49	17.06
C-20	Unflared	2	17.56	17.08
C-20	Unflared	3	17.63	17.25
C-20	Flared	1	17.21	17.14
C-20	Flared	2	17.50	17.23

Tooth	Time	Rep	DV	EM
C-20	Flared	3	17.47	17.27
C-20	Concluded	1	17.20	16.90
C-20	Concluded	2	17.28	16.91
C-20	Concluded	3	17.25	16.88
C-21	Unflared	1	19.08	18.60
C-21	Unflared	2	19.28	18.87
C-21	Unflared	3	19.35	18.78
C-21	Flared	1	19.19	18.67
C-21	Flared	2	18.81	18.69
C-21	Flared	3	18.93	18.89
C-21	Concluded	1	18.90	18.69
C-21	Concluded	2	18.69	18.68
C-21	Concluded	3	18.70	18.87
C-22	Unflared	1	19.15	18.60
C-22	Unflared	2	19.19	18.81
C-22	Unflared	3	18.98	18.86
C-22	Flared	1	18.83	18.65
C-22	Flared	2	18.96	18.71
C-22	Flared	3	18.97	18.97
C-22	Concluded	1	18.74	18.65
C-22	Concluded	2	18.76	18.63
C-22	Concluded	3	18.87	18.50
S-2	Unflared	1	20.07	19.83
S-2	Unflared	2	19.75	19.84
S-2	Unflared	3	19.96	20.03
S-2	Flared	1	20.00	19.98
S-2	Flared	2	20.00	19.89
S-2	Flared	3	19.91	19.83
S-2	Concluded	1	19.91	19.59
S-2	Concluded	2	19.84	19.49
S-2	Concluded	3	19.81	19.63
S-3	Unflared	1	17.58	17.64
S-3	Unflared	2	17.69	17.55
S-3	Unflared	3	17.81	17.71
S-3	Flared	1	17.32	17.62
S-3	Flared	2	17.46	17.63
S-3	Flared	3	17.51	17.50
S-3	Concluded	1	17.47	17.47
S-3	Concluded	2	17.62	17.44
S-3	Concluded	3	17.52	17.52
S-4	Unflared	1	20.72	20.24
S-4	Unflared	2	20.77	20.45
S-4	Unflared	3	20.85	20.62
S-4	Flared	1	20.77	20.34
S-4	Flared	2	20.72	20.27
S-4	Flared	3	20.76	20.61
S-4	Concluded	1	20.69	20.00
S-4	Concluded	2	20.48	20.09
S-4	Concluded	3	20.46	20.25
S-5	Unflared	1	19.37	19.11
S-5	Unflared	2	19.37	19.18
S-5	Unflared	3	19.45	19.16
S-5	Flared	1	19.25	19.16
S-5	Flared	2	19.39	19.15
S-5	Flared	3	19.24	19.00
S-5	Concluded	1	18.68	18.93
S-5	Concluded	2	18.65	18.98
S-5	Concluded	3	18.64	18.93
S-6	Unflared	1	19.09	19.07
S-6	Unflared	2	19.16	18.96
S-6	Unflared	3	19.33	19.09
S-6	Flared	1	19.27	18.83
S-6	Flared	2	19.30	18.87
S-6	Flared	3	19.20	18.84
S-6	Concluded	1	18.79	18.66
S-6	Concluded	2	18.71	18.68
S-6	Concluded	3	18.74	18.69
S-7	Unflared	1	19.91	19.53
S-7	Unflared	2	20.19	19.80
S-7	Unflared	3	19.74	19.89
S-7	Flared	1	19.84	19.53
S-7	Flared	2	19.76	19.51
S-7	Flared	3	19.72	19.45
S-7	Concluded	1	19.79	19.53
S-7	Concluded	2	19.83	19.29
S-7	Concluded	3	19.88	19.39
S-8	Unflared	1	21.61	21.46
S-8	Unflared	2	21.66	21.20
S-8	Unflared	3	21.38	21.24
S-8	Flared	1	21.67	21.13
S-8	Flared	2	21.58	21.43
S-8	Flared	3	21.64	21.31
S-8	Concluded	1	21.14	21.09
S-8	Concluded	2	21.07	20.96
S-8	Concluded	3	21.05	20.94
S-9	Unflared	1	22.16	22.05
S-9	Unflared	2	22.23	22.03
S-9	Unflared	3	22.17	22.13
S-9	Flared	1	22.27	21.97
S-9	Flared	2	22.31	22.26

Tooth	Time	Rep	DV	EM
S-9	Flared	3	22.40	22.11
S-9	Concluded	1	21.87	21.67
S-9	Concluded	2	21.78	21.70
S-9	Concluded	3	21.83	21.89
S-1	Unflared	1	20.09	19.87
S-1	Unflared	2	20.09	20.28
S-1	Unflared	3	19.94	20.23
S-1	Flared	1	19.82	19.87
S-1	Flared	2	19.87	19.89
S-1	Flared	3	19.77	19.90
S-1	Concluded	1	19.76	19.85
S-1	Concluded	2	19.65	19.50
S-1	Concluded	3	19.75	19.85
S-10	Unflared	1	19.35	19.18
S-10	Unflared	2	19.24	19.08
S-10	Unflared	3	19.26	19.27
S-10	Flared	1	19.48	19.43
S-10	Flared	2	19.49	19.38
S-10	Flared	3	19.64	19.43
S-10	Concluded	1	19.12	18.93
S-10	Concluded	2	19.03	19.05
S-10	Concluded	3	18.98	19.17
S-11	Unflared	1	18.47	18.33
S-11	Unflared	2	18.42	18.36
S-11	Unflared	3	18.27	18.36
S-11	Flared	1	18.34	18.21
S-11	Flared	2	18.52	18.32
S-11	Flared	3	18.55	18.28
S-11	Concluded	1	18.09	17.83
S-11	Concluded	2	18.07	18.02
S-11	Concluded	3	18.08	17.90
S-12	Unflared	1	19.24	19.05
S-12	Unflared	2	18.91	18.85
S-12	Unflared	3	19.13	19.08
S-12	Flared	1	19.26	19.06
S-12	Flared	2	19.42	18.97
S-12	Flared	3	19.38	19.02
S-12	Concluded	1	19.14	18.94
S-12	Concluded	2	19.03	19.07
S-12	Concluded	3	19.09	18.92
S-13	Unflared	1	19.19	18.91
S-13	Unflared	2	19.17	18.89
S-13	Unflared	3	19.28	18.81
S-13	Flared	1	19.16	18.73
S-13	Flared	2	18.99	18.84
S-13	Flared	3	19.23	18.82
S-13	Concluded	1	18.88	18.87
S-13	Concluded	2	18.82	18.81
S-13	Concluded	3	18.95	18.68
S-14	Unflared	1	16.38	16.20
S-14	Unflared	2	16.42	16.20
S-14	Unflared	3	16.34	16.19
S-14	Flared	1	16.54	15.83
S-14	Flared	2	16.65	15.76
S-14	Flared	3	16.45	15.81
S-14	Concluded	1	16.13	15.79
S-14	Concluded	2	15.97	15.70
S-14	Concluded	3	16.08	15.92
S-15	Unflared	1	17.50	17.18
S-15	Unflared	2	17.33	17.23
S-15	Unflared	3	17.45	17.08
S-15	Flared	1	17.26	16.67
S-15	Flared	2	17.45	16.85
S-15	Flared	3	17.25	16.97
S-15	Concluded	1	17.45	17.03
S-15	Concluded	2	17.11	16.98
S-15	Concluded	3	17.16	17.11
S-16	Unflared	1	18.89	18.78
S-16	Unflared	2	18.73	18.71
S-16	Unflared	3	18.73	18.87
S-16	Flared	1	18.43	18.52
S-16	Flared	2	18.27	18.51
S-16	Flared	3	18.46	18.49
S-16	Concluded	1	17.96	17.85
S-16	Concluded	2	18.08	17.65
S-16	Concluded	3	17.96	17.73
S-17	Unflared	1	19.16	18.93
S-17	Unflared	2	19.11	19.02
S-17	Unflared	3	19.15	19.14
S-17	Flared	1	19.06	19.11
S-17	Flared	2	19.24	18.89
S-17	Flared	3	19.17	18.90
S-17	Concluded	1	18.98	18.72
S-17	Concluded	2	19.01	18.80
S-17	Concluded	3	19.13	18.87
S-18	Unflared	1	20.53	20.43
S-18	Unflared	2	20.62	20.45
S-18	Unflared	3	20.63	20.34
S-18	Flared	1	20.92	20.20
S-18	Flared	2	20.70	20.28

Tooth	Time	Rep	DV	EM
S-18	Flared	3	20.64	20.28
S-18	Concluded	1	20.33	20.08
S-18	Concluded	2	20.31	20.18
S-18	Concluded	3	20.46	20.23
S-19	Unflared	1	19.73	19.01
S-19	Unflared	2	19.67	19.16
S-19	Unflared	3	19.59	19.23
S-19	Flared	1	19.36	18.83
S-19	Flared	2	19.25	18.86
S-19	Flared	3	19.49	18.89
S-19	Concluded	1	18.59	18.94
S-19	Concluded	2	18.65	18.67
S-19	Concluded	3	18.85	18.77
S-20	Unflared	1	16.36	16.38
S-20	Unflared	2	16.31	16.27
S-20	Unflared	3	16.54	16.25
S-20	Flared	1	16.41	16.75
S-20	Flared	2	16.30	16.70
S-20	Flared	3	16.21	16.52
S-20	Concluded	1	15.96	16.03
S-20	Concluded	2	16.20	16.04
S-20	Concluded	3	16.10	15.92
S-21	Unflared	1	17.58	17.52
S-21	Unflared	2	17.28	17.58
S-21	Unflared	3	17.49	17.39
S-21	Flared	1	17.59	17.37
S-21	Flared	2	17.70	17.44
S-21	Flared	3	17.63	17.41
S-21	Concluded	1	17.00	17.34
S-21	Concluded	2	16.98	17.52
S-21	Concluded	3	17.01	17.66
S-22	Unflared	1	16.46	16.29
S-22	Unflared	2	16.50	16.18
S-22	Unflared	3	16.46	16.22
S-22	Flared	1	16.11	15.98
S-22	Flared	2	16.28	15.92
S-22	Flared	3	16.24	15.91
S-22	Concluded	1	16.04	15.91
S-22	Concluded	2	16.06	15.89
S-22	Concluded	3	16.02	15.79
S-24	Unflared	1	16.77	16.52
S-24	Unflared	2	16.81	16.63
S-24	Unflared	3	16.73	16.79
S-24	Flared	1	16.62	16.42
S-24	Flared	2	16.83	16.55
S-24	Flared	3	16.83	16.57
S-24	Concluded	1	16.35	16.44
S-24	Concluded	2	16.37	16.33
S-24	Concluded	3	16.39	16.32

Vita

Dr. Mei I Tang was born on April 17, 1987 in Macau, China. She received her Bachelor of Science degree in Environmental Toxicology from the University of California, Davis in 2008, and her Doctor of Dental Medicine degree from the University of Pittsburgh School of Dental Medicine in 2014. After completion of a General Practice Residency at Allegheny General Hospital in Pittsburgh, she moved to Richmond, VA for an Endodontic Internship at Virginia Commonwealth University School of Dentistry. In 2016, Dr. Tang began her specialty training in the Advanced Dental Program in Endodontics at VCU. Dr. Tang is a member of the American Association of Endodontists, American Dental Association, and Virginia Dental Association. She will graduate with a Master of Science degree in Dentistry and a Certificate in Endodontics in June 2018.